EUROPEAN ORGANIZATION FOR NUCLEAR RESEARCH

CERN/ISRC/69-23
31 March 1969

INTERSECTING STORAGE RINGS COMMITTEE

AN ISOBAR EXPERIMENT FOR THE ISR

G.K. O'Neill

Palmer Physical Laboratory,
Princeton University, NJ, USA.

AN ISOBAR EXPERIMENT FOR THE ISR

G.K. O'Neill,
Palmer Physical Laboratory, Princeton University, NJ, USA.

1. INTRODUCTION

For the first operating period at the ISR, when the circulating beam currents may be low and the vacuum may not be very good in the interaction straight sections, it will still be possible to do several good experiments. This proposal describes an apparatus which is simple, inexpensive, and can realistically be built and made to work in the $2\frac{1}{2}$ years between now and the operation of the ISR. It can measure isobars down to cross-sections as low as 10 μb with only 0.1 ampere of beam in each ring (approximately one or two pulses from the PS), and can operate with a vacuum as poor as 10^{-9} instead of the eventual 10^{-11} for which the ISR straight sections are being designed.

2. TECHNIQUE

The idea of this experiment is contained in four observations, the first two of which are on physics and the last two on method.

1) In the decay of all known isobars, substantial transverse momentum is given to the decay products, and in a useful fraction of all events this momentum is adequate for bringing the particles into an apparatus that is made to approach the vacuum chamber closely in the vertical direction.

2) Isobar production at the energy of the PS is a considerable part of the total cross-section, and at the ISR energy there will almost surely be many isobars with production cross-sections of a few microbarns or more.

3) There exists an exact solution of Maxwell's equations that permits the construction of a magnetic field that is non-zero outside a rectangular boundary but zero inside it.

4) The known performance of magnetic-field optical spark chambers, tested in many experiments, is such that in a mirrorless optical system, systematic errors can be kept to the 0.1 mm range over a path length of several metres. Single-gap spark scatter is about 0.28 mm.

3. PLAN

The experiment is designed to detect low multiplicity forward-angle events, such as isobars decaying by the modes

$$n + \pi^+ , \quad p + \pi^+ , \quad p + \pi^+ + \pi^- , \quad n + \pi^+ + \pi^+ + \pi^- , \quad \text{etc.}$$

These are reactions with not more than one neutral in the final state. For reactions $n + \pi^+$, $p + \pi^+$, $p + \pi^+ + \pi^-$, and certain others, the measurement will be considerably overconstrained, leading to smaller total errors and better background rejection (see Appendix 8).

Particles heading toward the isobar spectrometer exit from the vacuum chamber at ℓ = 2.5 m (2.5 m from the interaction diamond; see Fig. 1) through a 3 mm stainless-steel spherical dome. Their scattering gives them typical transverse momentum errors of only 8 MeV/c, compared to 20 MeV/c for the beam particles. For clarity we now consider the $n + \pi^+$ decay mode. The angle error in scattering is 0.29 mrad for a 28 GeV/c particle, compared to 0.5 mrad for the beam protons. An outcoming π^+ passes through spark chambers 1 and 2, where its direction is measured in both coordinates to ±0.5 mrad. Its approximate direction is also measured by Charpak counter planes A and A', feeding logic that triggers on a single charged particle coming from the interaction region. The π^+ then goes through the 1 cm aluminium coil of the magnet, where its scattering no longer matters. (That scattering is, however, quite small, being only 0.24 mrad at 28 GeV/c.) The energy loss is 4.4 MeV and the Landau straggling leads to a 1 MeV/c momentum error contribution independent of energy. The π^+ then traverses five spark chambers over 5 metres of 3 kG field, acquiring a typical sagitta of 1 cm to 5 cm. In the isobar spectrometer magnet, only the vertical coordinate is measured, by direct photography without field lenses or mirrors.

The neutron passes through the entire apparatus including the 5 cm thick (0.17 nuclear mean free path) back coil of the magnet, and enters a 16-gap spark chamber made of 3.8 cm (0.10 nmfp) carbon plates. Here the position of the nuclear shower origin is measured to about ±0.5 cm in the plane normal to the beam, constituting a ±0.5 mrad direction measurement. For $n + \pi^+$ decay modes in single-isobar production, the direction measurements alone are sufficient for a 1C fit to isobar mass, (an observation due to B.D. Hyams).

In the backward direction (i.e. downstream for the opposing beam) the vacuum chamber flare is of the same diameter but the exit window is at ℓ = 7.5 metres, permitting the acceptance of particles down to 4 mrad. A pair of direction-measuring chambers, identical to SC's 1 and 2, and Charpak counters identical to A and A', measure the direction of an outcoming proton; a neutron detector, identical to B, measures neutron shower origin position in the case of charge transfer processes such as $p + p \rightarrow n + I^{++}$, where I^{++} is a doubly-charged isobar.

4. THE ISOBAR-SPECTROMETER MAGNET

The magnet has a field volume of 1.4 m × 1.4 m × 5 m, and runs at only 3 kG. Basically, it is a rectangular single-layer solenoid inside a steel box open at both ends. The field is horizontal, transverse to the beam-direction, and almost perfectly uniform. The beam pipe runs inside a 5-metre-long rectangular iron channel 1 cm thick, and the main magnet coils are wound in such a way as to make the field zero everywhere within the channel. There is also no fringe field outside the magnet. The total magnet weight is only 40 tons, and the power is only 1 MW. The magnet accepts angles down to 14 mrad, and up to 165 mrad.

Two possible variations of the isobar spectrometer magnet design have been considered; the first is a doubling of power, coil weight, and magnetic field, with an increase of a factor of 2.3 in iron weight. It is probably not worth while, because for our position-measuring errors a BL^2 of 150 kG-m^2 would lead to Δp errors of 170 MeV/c or less for $p < 22$ GeV/c, which would make the beam momentum errors (170 MeV/c) dominant at all momenta in the isobar decay range (see Appendix 8). Further, the price of this marginal gain would include a loss of 3 mrad in minimum angle. A

second variation may be more worth while; it is an increase of spectrometer height to 2.0 m. For two-body decays of the highest known isobars (e.g. the 2850) this variation would improve acceptance by a factor of 1.6, at the expense of about 30% higher cost for the magnet. The choice is not critical and will be made after more detailed Monte Carlo calculations on three- and four-particle isobar decays. A half-scale, full-field model of a 60 cm length of the magnetic channel and its surrounding uniform-field region is being made at Princeton to demonstrate the practicality of the zero-field-channel solution. The magnet is so simple and inexpensive that it can be designed and, if necessary, built without recourse to CERN personnel or funds, but it may be best from the viewpoint of laboratory policy to have such a generally useful device built as CERN equipment.

We would like to complete the apparatus about one year before ISR operation and use it for isobar detection at the PS, with a liquid-hydrogen target. Outcoming particle angles and acceptances would be identical to the ISR case in the peripheral approximation.

The appendices which follow include calculations of optical errors, measuring errors, magnet properties, scattering effects, data-taking rates, isobar acceptances, backgrounds, and mass resolution.

APPENDIX 1

ISOBAR ACCEPTANCES

As will be shown in the following appendices, any particle entering the magnet and traversing half or more of it will have its momentum measured with acceptably small errors. A Monte-Carlo program was therefore run with a cut made for simplicity of the optics: the entire median-plane region was thrown away; therefore the required angle of elevation relative to the median plane was $|\theta_{el}| > 14$ mrad. A pion trajectory was required to enter the magnet with acceptable θ_{el} and traverse at least half of it. The neutron was required to satisfy the same entrance requirement but to traverse all of the magnet. The decay mode Isobar $\rightarrow$ $n + \pi^+$ was studied for several values of isobar mass m_I, assuming isobar production with a gaussian distribution in p_T, with half-width 300 MeV/c. We assumed a minimum four-momentum transfer, and isotropic isobar decay. The fraction of all isobars detected is given in Table 1. The numbers are the fraction of isobars accepted on the right once the "struck" proton is accepted on the left.

Table 1

Isobar acceptances

m_I MeV	Fraction accepted assuming 1.4 m magnet height %	Fraction accepted assuming 2.0 m magnet height %
1200	20	20
1400	43	43
1600	50	53
2000	52	61
2600	33	54
3000	13	26
3400	6	14
4000	0	5

Clearly the larger magnet would be preferable only for high values of m_I, as is reasonable. All the acceptances are large enough for good measurements of production cross-sections.

APPENDIX 2

BACKGROUND

For conservatism we assume that although the experimental straight sections are designed for an eventual vacuum of 10^{-11} mm, they begin with the same vacuum as the rest of the ring, i.e. 10^{-9} mm. The proposed experiment can be done with circulating currents as small as 2×10^{12} protons, the equivalent of one or two pulses from the PS.

The beam lifetime is about one day and the losses are assumed distributed uniformly around the rings. The rate of beam-gas interactions per 10 metres of length is therefore

$$R = 2 \times (2 \times 10^{12}) \times \left(\frac{10}{1000}\right) \times 10^{-5} = 4 \times 10^{5} = 1/2.5\ \mu\text{sec}$$

↑ 2 beams; ↑ circumference; ↖ $(\text{lifetime})^{-1}$

A d.c.-powered veto counter connected to dead-time-less d.c. logic will accept events only when no interaction has occurred in the previous microsecond (the approximate clearing time). The delay time before spark chamber firing will be about 0.4 μsec, so the probability of a beam-gas interaction appearing in a picture will be 0.4 μsec/2.5 μsec = 15%.

We emphasize that the numbers are equally favourable for a twenty-ampere circulating current, as long as the improvement in ISR local vacuum keeps pace with the improvement in ISR beams.

APPENDIX 3

COUNTING RATE

For the initial experiment we trigger on interactions from which one neutral and one charged particle enter the main apparatus, a single charged particle goes to the opposing-beam detector, and no other particles are produced. The resulting triggers will probably be about 10% of the total inelastic cross-section, or 2 mb. They may in fact be mainly isobars, but we do not depend on that. One trigger per 5 seconds is an adequate data-taking rate, so we require a luminosity

$$\mathcal{L} = \mathcal{L}_0 \left(\frac{0.2/\text{sec}}{1.6 \times 10^5/\text{sec}} \right) \left(\frac{40 \text{ mb}}{2 \text{ mb}} \right) = 2.5 \times 10^{-5} \quad \mathcal{L}_0 = \frac{\mathcal{L}_0}{4 \times 10^4} \ .$$

We can reach this luminosity with 1/200 of the nominal ISR current, that is 0.1 ampere in each beam. In a 400 hour run we collect 290,000 pictures, and in these a resonance with a 10 μb cross-section will show up with

$$N = 290{,}000 \left(\frac{10 \, \mu\text{b}}{2 \text{ mb}} \right) (0.3) \ (0.4) = 170 \text{ events} \ .$$

The factor 0.3 is inserted as the minimum acceptance of the isobar spectrometer for extreme values of m_I, and 0.4 is the fraction of "struck" 28 GeV protons which escape the pipe.

We note therefore that even with 1/200 of the nominal ISR current and a vacuum 100 times worse than the design value, we should be able to measure isobar cross-sections and angular distributions down to cross-section values that are as low as those of good present-day PS experiments.

APPENDIX 4

SPARK JITTER AND MULTIPLE SCATTERING ERRORS

a) The vacuum chamber exit window is taken to be stainless steel, because it can then be easily welded to the 6 cm × 15 cm chamber that continues downstream. The welded joint is at a critical position for minimum-angle coverage, and the use of a more exotic window material would probably require a more bulky joint.

Throughout this discussion we use the formula

$$\theta_{rms} = \frac{21}{E(MeV)} \sqrt{\frac{L}{L_{rad}}} ,$$

which overestimates the scattering by omitting the Moliere correction. For momenta below 20 GeV/c this means our resolution is about 30% better than the number we use here. For the vacuum chamber window, $L/L_{rad} = 0.165$, and at 28 GeV $\theta_{rms} = 0.29$ mrad. This gives an 8 MeV/c contribution to the transverse momentum errors, compared to 20 MeV/c inherent in the ±0.5 mrad random angles of each of the two beam protons. The transverse momentum error introduced by the window is

$$\Delta p_T = \theta_{rms} E = 8 \text{ MeV independent of } E .$$

b) The spark jitter for conventional narrow-gap spark chambers in a magnetic field is ±0.28 mm. Each of the chambers 1-7 has 16 gaps, and experience has shown that, at least up to that number of gaps, the errors reduce statistically as $1/\sqrt{n}$. The spark-jitter error contribution is therefore $0.28 \text{ mm}/\sqrt{16} = 0.07 \text{ mm} = \Delta Z_j$ at each chamber.

The particle direction measurement is done by chambers 1 and 2, in 90° stereo. In the absence of optical errors, the angle accuracy would be

$$\theta_{12} = \frac{(0.07 \text{ mm})\sqrt{2}}{650 \text{ mm}} = \frac{1}{6500} = 0.15 \text{ mrad} .$$

However, these chambers are viewed through mirrors, so we assume the accuracy is much worse; it can be as bad as 0.5 mrad without contributing much to over-all transverse momentum errors. In the side view, the systematic error in SC2 due to mirrors can be corrected for by following tracks through the adjacent and mirrorless chamber No. 3.

c) On passage through the thin-window portion of the magnet, that is 1 cm of Al, the scattering angle is important only for the particles of minimum angle, because by a trick we avoid having to lose the dead region of SC3 closest to the median plane, and thus gain 3 mrad. The trick is to measure at the centre of No. 2. That measurement is fuzzed by an amount

$$\Delta Z = \theta_w \, (\ell_w - \ell_2) \ ,$$

where θ_w is the coil-window scattering and $(\ell_w - \ell_2) = 13$ cm. Then

$$\Delta Z = \frac{21}{E} \sqrt{\frac{1}{8.9}} \, (130) = 0.033 \text{ mm} \left(\frac{28}{E}\right) \ ,$$

which is negligible for all energies down to 4 GeV. The effective start-point for the sagitta measurement is therefore the front coil; if this technique is followed for particles at all angles, it can be argued that chamber No. 3 is present only for redundancy and to calibrate chamber No. 2. We do <u>not</u> assume the use of this method in the calculations that follow. One should note also that the start and the end-point measurement errors can be a factor of two worse than those at the centre-point before contributing equally to the sagitta error.

d) Spark chambers Nos. 4 and 6 are present, not to improve momentum accuracy on long tracks, but to permit good measurements on particles going only half or three-quarters of the way through the magnet. We therefore treat the momentum measurement as if done by only three chambers, 3, 5, and 7. Outside the spark chambers, the magnet is flooded with helium. The scattering is therefore dominated by the aluminium and neon of chamber No. 5. For that chamber

$$\left(\frac{L}{L_{rad}}\right)_1 = \underset{\text{plates}}{17} \times 0.0025 \text{ cm} \times 1/8.9 \text{ cm} = 0.0048 \quad \text{(aluminium)}$$

$$\left(\frac{L}{L_{rad}}\right)_2 = \underset{\text{gaps}}{16} \times 1.2 \text{ cm} \times \left(\frac{36}{30}\right) \times \frac{30}{20} \times \frac{1}{3 \times 10^4 \text{ cm}} = 0.00115 \quad \text{(neon)} \ .$$

We include also a 5-metre length in helium as if concentrated at SC5:

$$L_{rad}(He) = \frac{85 g/cm^2(He)}{36 g/cm^2(air)} \times \frac{28}{4} \times 3 \times 10^4 \text{ cm} = 5 \times 10^5 \text{ cm} ,$$

thus

$$\left(\frac{L}{L_{rad}}\right)_3 = \frac{500}{5 \times 10^5} = 0.001 .$$

In total, then,

$$\left(\frac{L}{L_{rad}}\right)_{total} = 0.0048 + 0.0011 + 0.001 = 0.0069 ,$$

and

$$\theta_{rms} = \frac{21}{E}\sqrt{0.0069} = \frac{1.7}{E(MeV)} = 0.6 \times 10^{-4} = 0.06 \text{ mrad at 28 GeV/c} .$$

For a total track length 2y, a scattering at the centre produces an uncertainty $\theta_{rms}\, y = \Delta Z_s$ at the end point; this is

$$\Delta Z_s = \theta_{rms}\, y = (0.6 \times 10^{-4} \text{ mrad})\ (2.3 \text{ m}) = 0.138 \text{ mm}$$

at 28 GeV.

e) The spark-jitter error at each chamber is compounded with the errors of the automatic measuring machine (HPD, PATR, etc.). The latter are discussed in another appendix, but the result is, for HPD errors of ± 1.5μ and a magnification of 50, a measuring error

$$\Delta Z_m = 0.0015 \text{ mm} \times 50 = 0.075 \text{ mm} .$$

We assume, pessimistically, that this is a systematic HPD error which is not reduced by measurement of 16 sparks. We therefore compound it with the final 0.07 mm spark-jitter error of a 16-gap spark chamber.

f) Summarizing,

$$\text{Start-point error} = \sqrt{\Delta Z_j^2 + \Delta Z_m^2} = \sqrt{(0.07)^2 + (0.075)^2} =$$

$$= \sqrt{110 \times 10^{-4}} = 0.105 \text{ mm} = \Delta Z_3 .$$

The mid-point error is the same (ΔZ_5).

The end-point error is

$$\sqrt{\Delta Z_j^2 + \Delta Z_m^2 + \Delta Z_s^2} = \sqrt{(110 + 196) \times 10^{-4}} = 0.175 \text{ mm} = \Delta Z_7 .$$

g) The sagitta error ΔS depends on ΔZ_5 directly; the end-point errors enter with a factor $\frac{1}{2}$:

$$\Delta S = \sqrt{\left(\frac{\Delta Z_3}{2}\right)^2 + (\Delta Z_5)^2 + \left(\frac{\Delta Z_7}{2}\right)^2} = \sqrt{(0.052)^2 + (0.105)^2 + (0.086)^2}$$

$$= \sqrt{(27 + 110 + 74) \times 10^{-4}} = 0.15 \text{ mm} .$$

Most of the isobar-decay pions will have much less than the full energy, but we consider the sagitta of a 28 GeV/c proton anyway; we assume only a 4.6 m effective length, meaning that we depend only on chambers Nos. 3, 5, and 7, <u>not</u> on No. 2.

$$BR = (33 \text{ kG-m/GeV/c}) \ (28 \text{ GeV/c}) = 920 \text{ kG-m} .$$

$$R = 920/3 = 306 \text{ m} .$$

The sagitta $$S = \frac{y^2}{2R} = \frac{(2.3 \text{ m})^2}{612 \text{ m}} = 8.5 \text{ mm} .$$

The momentum errors on a full-energy proton will therefore be (see Fig. 2)

$$\Delta p/p = 0.15 \text{ mm}/8.5 \text{ mm} = 1.8\% .$$

In event reconstruction, the total longitudinal errors including those of the beam will be (for a 28 GeV/c proton)

$$\Delta p_L = \sqrt{(0.17)^2 + (0.50)^2} = 0.53 \text{ GeV/c} .$$

For the 5-15 GeV/c region typical of an isobar decay pion, the error will be less than 1%, giving a Δp_L less than that of the circulating proton beams (see Fig. 2). For this proposal we have assumed quite pessimistic values for scattering and for measuring errors; a model is being made to test optical and measuring errors.

APPENDIX 5

OPTICAL AND MEASURING ERRORS

For a depth of field Δy, the reprojected spot diameter is (at extreme depth) $d_1 = \Delta y/MF$, where M is the magnification and F the camera f-number. Diffraction contributes a spot diameter

$$d_2 = 1.22\lambda\ (MF)\ .$$

Minimizing these contributions for Δy = 700 mm and λ = 6000 Å, we find an optimum MF product of 950. However, we choose to work off-optimum at MF = 550 in order to ease the requirements on the automatic measuring system. The optical parameters are:

Focal length = 30 cm Object distance = 15 metres
M = 50 F = 11 (single camera)
Film format: 35 mm unperforated film
28 mm × 100 mm block size.

The apparent reprojected spark widths for a typical 1.2 mm spark will then be:

Central focal plane:	1.3 mm
Half-way to full depth:	1.4 mm
Extremes:	1.8 mm.

We assume for the measuring machines a systematic error of ±1.5 μ over a distance of 2 mm to 4 mm between sparks and fiducials. This pessimistic value corresponds to 1.5 μ × 50 = 0.075 mm reprojected, which is the value assumed in Appendix 4.

The fiducials will be anchored to the 2 m × 5 m × 15 cm steel backplate of the magnet. Their apparent size will be 1.3 mm, about the same as a spark.

APPENDIX 6

MAGNET

In this section, a number in parentheses refers to the 2-metre-height version of the magnet, shown in Fig. 1.

Clear length:	5.0 metres	
Inside width:	1.4 metres	
Inside height:	1.4 metres	(2.0 m)
Iron thickness:	15 cm	(22 cm)
Aluminium weight:	2.5 tons	(2.8 tons)
Iron weight:	37 tons	(65 tons)
Total weight:	40 tons	(68 tons)
Inner aperture stop:	elevation-angle ±5 cm at 3.5 m; 14.3 mrad.	
Power:	1.0 MW	(1.11 MW)
Entrance window:	82 cm × 82 cm	(82 cm × 122 cm)

APPENDIX 7

MAGNET MODEL

The unusual feature of the magnet is its provision of uniform field over a large volume but zero field inside a rectangular boundary. To illustrate this concept a model is being built, half size, with full field in the iron, of a 60 cm length of the zero-field channel and its immediate surrounding uniform-field region. This will include the end region. The magnet model is shown in Fig. 3, which also illustrates the solution of the field equations.

APPENDIX 8

ISOBAR MASS ERRORS

The purposes of pion momentum measurement are to permit the study of a much larger class of decay modes than the $n + \pi$, and incidentally to improve mass resolution and reduce background. We illustrate the second point in the following discussion.

It was observed by B.D. Hyams that an isobar mass measurement can be made from direction information alone. That approach leads to the formula

$$m_i = \sqrt{m_\pi^2\left(1 + \frac{\theta_\pi}{\theta_n}\right) + m_n^2\left(1 + \frac{\theta_n}{\theta_\pi}\right) + p_p^2\,\theta_\pi\theta_n}$$

in the small-angle, extreme relativistic limit, where θ_π and θ_n are both measured from the negative-extended line of the opposing-beam proton, and p_p is the momentum of a beam proton. In the last term, p_p enters squared, so its 0.6% error gives 1.2%. The transverse-momentum uncertainty in the beams (20 MeV/c) makes the reference line uncertain by 0.02/28 = 0.72 mrad. θ_n is often small. For the 1300 MeV mass region, the angle error contributes 5% to the last term in the best case, the total mass resolution then being about 1% (12 MeV). In the case of the isobar spectrometer, with measurement of neutron direction and pion momentum, the corresponding formula is

$$m_i = \sqrt{m_\pi^2(p_p/p_\pi) + m_n^2\,p_p/(p_p - p_\pi) + p_\pi(p_p - p_\pi)\,(\theta_n + \theta_\pi)^2}$$

In the last term, errors in p_π contribute 0.6%, in p_p 0.9%, and in angle measurement 1.6%. Most importantly, the dependence on beam transverse momentum uncertainty has vanished to first order. The total mass resolution is then 0.4% (5 MeV). Note also that for pion momenta of the order of 15 GeV/c, the isobar mass becomes less sensitive to p_π; this is a reason why there may not be much point in further improvements of momentum resolution beyond the values we can achieve with this simple apparatus.

ISOBAR PRODUCTION EXPERIMENT (ISR)

(14-200 MILLIRADIANS)

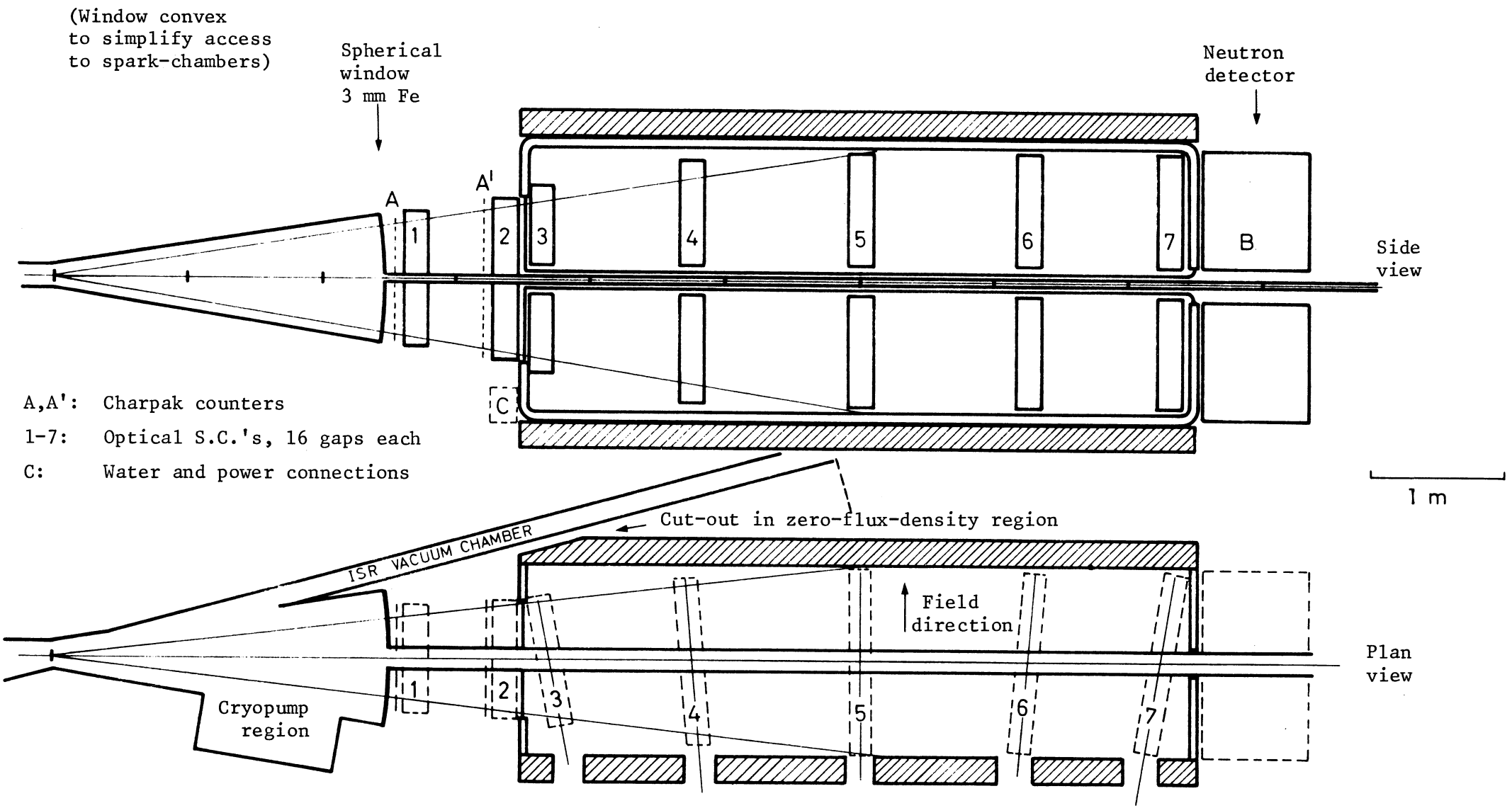

MAGNET: 65 tons steel OR 37 tons steel
2.8 tons Al 2.5 tons Al
1.1 MW power 1.0 MW power
(shown above) (same in plan view)

Fig. 1

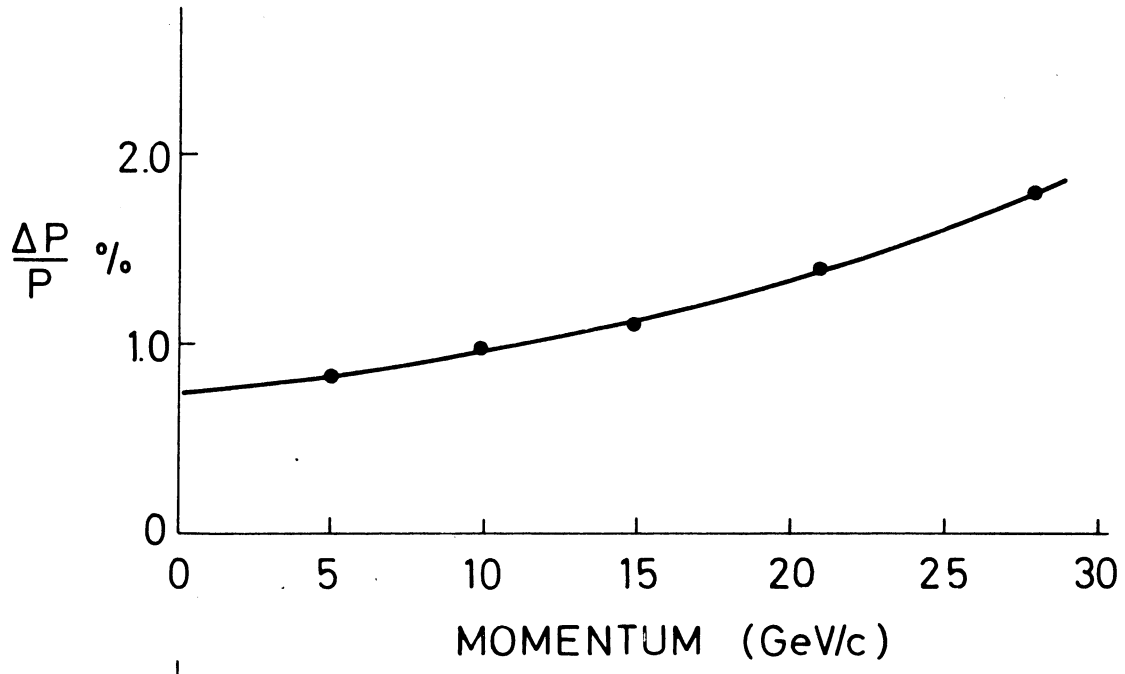
2.0
ΔP/P %
1.0
0
0
5
10
15
20
25
30
MOMENTUM (GeV/c)

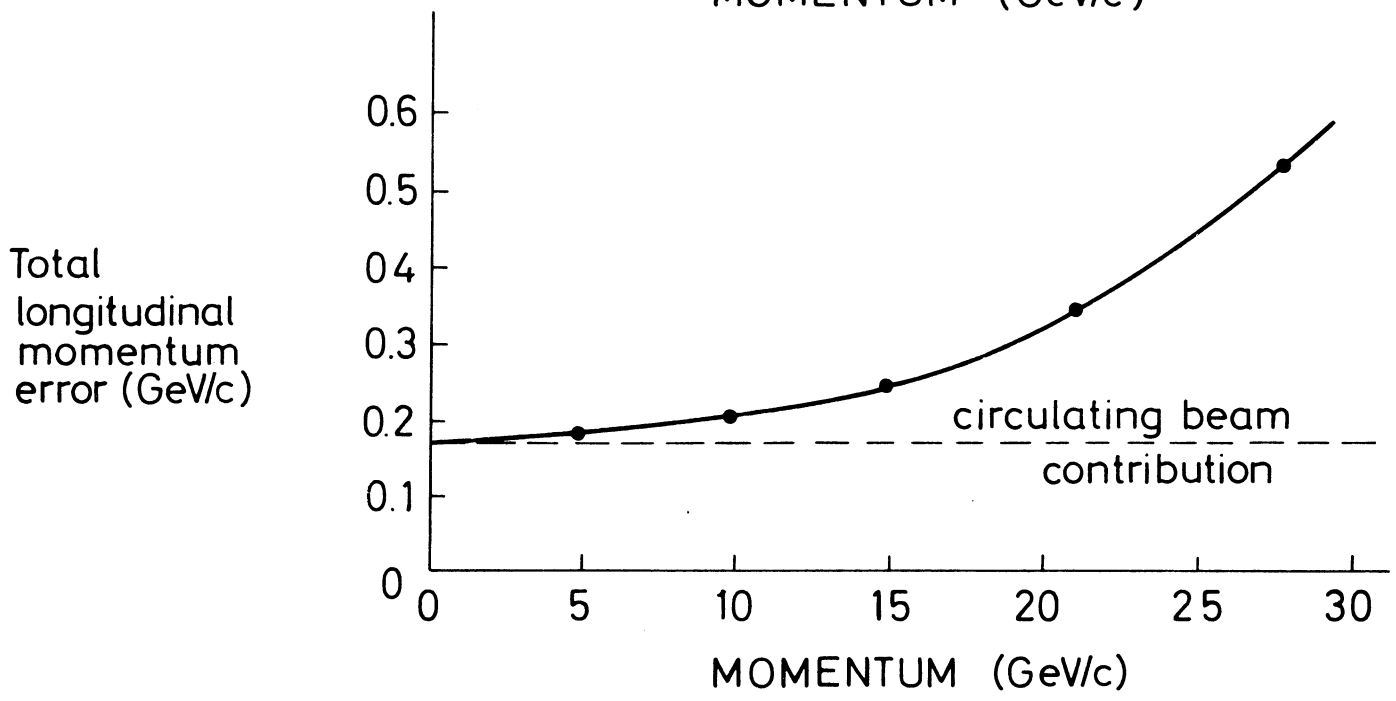
Total longitudinal momentum error (GeV/c)
0.6
0.5
0.4
0.3
0.2
0.1
0
circulating beam contribution
0
5
10
15
20
25
30
MOMENTUM (GeV/c)

FIG.2

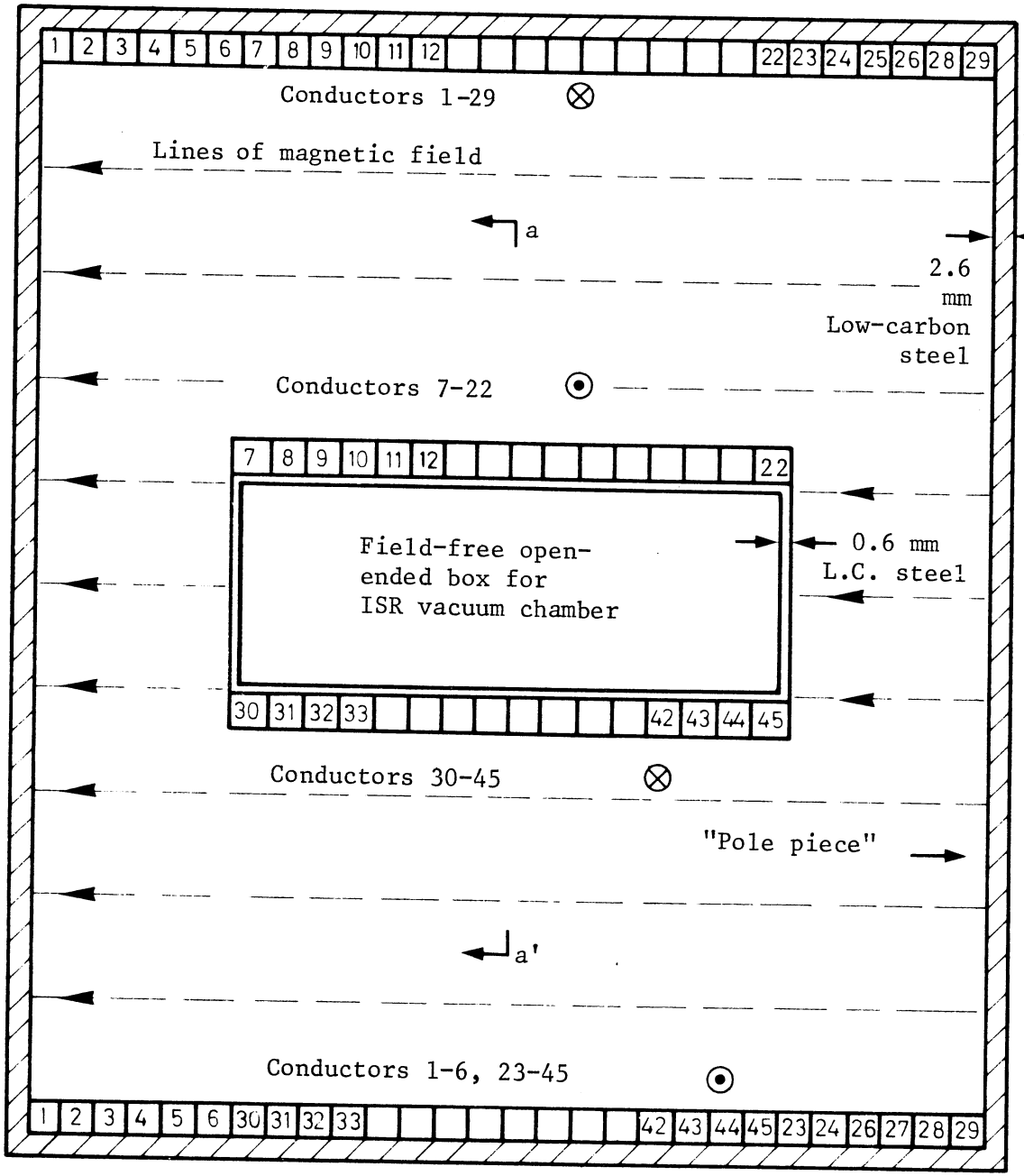

Return yoke

End view (Section bb')

Half-scale magnet model shown full size. Field in air: 500 gauss. Field in iron: 15 kG. Central box and conductors are to correct half-scale except that iron is made only 0.6 mm thick, ∴ runs at 15 kG.

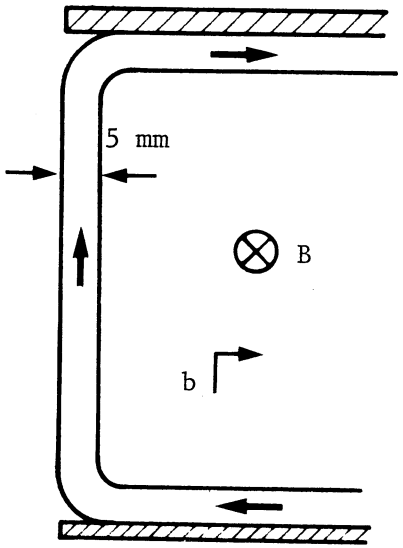

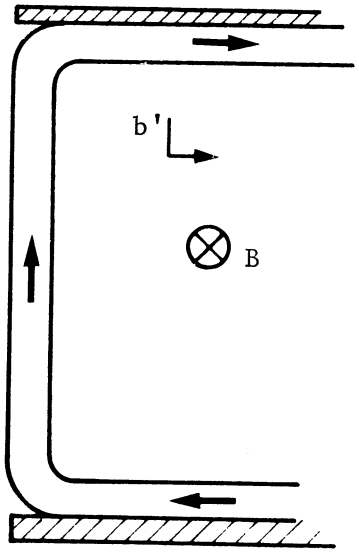

Side view (Section aa')

Fig. 3